CDF note 7635

First Measurement of the Ratio of Branching Fractions $\mathcal{B}(\Lambda_b \to \Lambda_c^+\mu^-\overline{\nu}_\mu)/\mathcal{B}(\Lambda_b \to \Lambda_c^+\pi^-)$

The CDF Collaboration

URL http://www-cdf.fnal.gov

(Dated: October 17, 2008)

This note presents the first measurement of the ratio of branching fractions $\mathcal{B}(\Lambda_b \to \Lambda_c^+\mu^-\overline{\nu}_\mu)/\mathcal{B}(\Lambda_b \to \Lambda_c^+\pi^-)$. In addition, measurements of $\mathcal{B}(\overline{B}^0 \to D^+\mu^-\overline{\nu}_\mu)/\mathcal{B}(\overline{B}^0 \to D^+\pi^-)$ and $\mathcal{B}(\overline{B}^0 \to D^{*+}\mu^-\overline{\nu}_\mu)/\mathcal{B}(\overline{B}^0 \to D^{*+}\pi^-)$ are made and serve as control samples to cross-check our analysis methods. Using approximately 172 pb^{-1} of data from $p\overline{p}$ collisions with a center of mass energy $\sqrt{s} = 1.96$ TeV taken with the CDF-II detector, the relative branching fractions are measured to be:

$$\frac{\mathcal{B}(\Lambda_b \to \Lambda_c^+\mu^-\overline{\nu}_\mu)}{\mathcal{B}(\Lambda_b \to \Lambda_c^+\pi^-)} = 16.6 \pm 3.0\ (stat) \pm 1.0\ (syst)^{+2.6}_{-3.4}\ (PDG) \pm 0.3\ (EBR),$$

$$\frac{\mathcal{B}(\overline{B}^0 \to D^+\mu^-\overline{\nu}_\mu)}{\mathcal{B}(\overline{B}^0 \to D^+\pi^-)} = 9.9 \pm 1.0\ (stat) \pm 0.6\ (syst) \pm 0.4\ (PDG) \pm 0.5\ (EBR),$$

$$\frac{\mathcal{B}(\overline{B}^0 \to D^{*+}\mu^-\overline{\nu}_\mu)}{\mathcal{B}(\overline{B}^0 \to D^{*+}\pi^-)} = 16.5 \pm 2.3\ (stat) \pm 0.6\ (syst) \pm 0.5\ (PDG) \pm 0.8\ (EBR).$$

The uncertainties are from statistics (stat), CDF internal systematics(syst), world averages of measurements published by the Particle Data Group or subsidiary measurements in this analsysis (PDG) and unmeasured branching fractions estimated from theory (EBR), respectively. As part of this analysis, measurements of the branching fractions of four new Λ_b decays: $\Lambda_b \to \Lambda_c(2595)^+\mu^-\overline{\nu}_\mu$, $\Lambda_b \to \Lambda_c(2625)^+\mu^-\overline{\nu}_\mu$, $\Lambda_b \to \Sigma_c(2455)^0\pi^+\mu^-\overline{\nu}_\mu$ and $\Lambda_b \to \Sigma_c(2455)^{++}\pi^-\mu^-\overline{\nu}_\mu$ relative to the branching fraction of the $\Lambda_b \to \Lambda_c^+\mu^-\overline{\nu}_\mu$ decay are presented. The measured the transverse-momentum distribution of Λ_b baryons is found to be significantly different from the transverse-momentum distribution of $\overline{B}^0$ mesons produced from $\overline{p}p$ collisions. This difference in production spectra results in a modification of the production cross section ratio, $\sigma_{\Lambda_b}/\sigma_{B^0}$, with respect to the CDF I measurement.

I. INTRODUCTION

Much of the physics which describes the decay of a b flavored hadron may be understood from the the branching ratio of that b hadron to a specific final state. A b hadron is a bound state of either three quarks (baryon) or a quark-antiquark pair (meson) with one b quark (or antiquark). A branching ratio is the ratio of the rate at which a specific initial particle decays to a specific final state compared to the total rate of decay of that particle. The decay rate being proportional to the square of the quantum mechanical amplitude describing the decay. According to the standard model of particle physics, amplitudes for the weak decays of b hadrons are described as the product of Cabibbo-Kobayashi-Maskawa (CKM) coupling strengths [1, 2] and dynamical factors. In order to extract the CKM coupling strengths, knowledge of the dynamical factors is needed from either experiment or theory. Calculation of these dynamical factors, in the case of b hadron decays is aided by heavy quark effective theory (HQET). In HQET, the b hadron is treated similar to an atom where the heavy b quark ($m_b \approx 4$ GeV/c^2), plays a similar role as the nucleus and the light quarks ($m_{u,d,s} < 100$ MeV/c^2) are treated similar to electrons [3–5]. In ground state b mesons, one treats the interaction between the spins of the b quark and the light ($\overline{u}$, $\overline{d}$, $\overline{s}$) antiquarks as a correction to the basic interaction. For the ground state b baryons, the two light quarks have a total relative angular momentum of zero. One ground state b meson is called $\overline{B}^0$ (containing $b\overline{d}$) and one ground state b baryon is called Λ_b (containing u, d, b quarks). With the angular momentum of the a ground state b baryon coming solely from the b quark, predictions for branching fractions for ground state baryon decays are simpler compared with similar calculations for mesons. However, much less is known experimentally about b baryons than b mesons. At the time of writing this article, only five decay modes of the Λ_b^0 baryon have been observed and have large uncertainties on their branching fraction measurements. Hundreds of branching ratios have been measured for the B^0. At present, b baryons are only produced in $\overline{p}p$ collisions at the Fermilab Tevatron and may be detected by the CDF or Dzero experiments. Using HQET, Huang, *et al.* [6] and Leibovich, *et al.* [7] calculate $\mathcal{B}(\Lambda_b \to \Lambda_c^+\mu^-\overline{\nu}_\mu)$ to be and $\mathcal{B}(\Lambda_b \to \Lambda_c^+\pi^-)$, respectively. Combining the above calcuations with particle property information summarized by the particle data group [8] the ratio of $\mathcal{B}(\Lambda_b \to \Lambda_c^+\mu^-\overline{\nu}_\mu)$ to $\mathcal{B}(\Lambda_b \to \Lambda_c^+\pi^-)$ is predited to be ∼14 with a 30% theoretical uncertainty.

This article presents the first measurements of the ratio $\mathcal{B}(\Lambda_b \to \Lambda_c^+\mu^-\overline{\nu}_\mu)/\mathcal{B}(\Lambda_b \to \Lambda_c^+\pi^-)$. In addition, we make similar measurements in the $\overline{B}^0$ system: the ratio $\mathcal{B}(\overline{B}^0 \to D^+\mu^-\overline{\nu}_\mu)/\mathcal{B}(\overline{B}^0 \to D^+\pi^-)$, and the ratio $\mathcal{B}(\overline{B}^0 \to D^{*+}\mu^-\overline{\nu}_\mu)/\mathcal{B}(\overline{B}^0 \to D^{*+}\pi^-)$. The $\overline{B}^0$ measurements serve as control samples to cross-check our analysis methods. The analysis strategy is as follows: we first reconstruct signals in the data. For the semileptonic mode, several backgrounds exhibit a similar signature to the real signal. We estimate the amount of these backgrounds ($N_{\rm bg}$) and subtract them from the observed yield in the data. Then, we obtain the detector acceptance and reconstruction efficiency (ϵ) from a Monte Carlo simulation (MC) of the Λ_b production, decay and the CDF-II detector. The Λ_b ($\overline{B}^0$) relative branching fraction is the yield ratio divided by the efficiency ratio since the numbers of b-hadrons cancel:

$$\frac{\mathcal{B}_{\rm exclsemi}}{\mathcal{B}_{\rm had}} = (\frac{N_{\rm inclusive\ semi} - N_{\rm bg}}{N_{\rm had}}) \times \frac{\epsilon_{\rm had}}{\epsilon_{\rm exclsemi}}. \tag{1}$$

II. DATA SAMPLE & EVENT SELECTION

This analysis is based on an integrated luminosity of 172 pb^{-1} collected with the CDF-II detector between February 2002 and September 2003. The CDF-II detector is described in detail elsewhere [9]. The data are derived from the "Two Track" Silicon Vertex Trigger (SVT) [10]. The "Two Track" SVT requires a pair of opposite charged tracks to satisfy the following requirements: for each track, the transverse momentum, P_T threshold of 2 GeV/c, an impact parameter, d_0, within 120 μm and 1000 μm. The impact parameter is the distance of closest approach between the track and the beam line in the $r\phi$ plane [11]. For the track pair, the azimuthal angle difference for the two track must be between 2° and 90°, and the decay length in the $r\phi$ plane ($L_{r\phi}$), must be larger than 200 μm. The decay length is distance between the two-track vertex and the beam line measured in the $r\phi$ plane. The "Two Track" SVT distinguishes b-hadron decays from other physics processes. The $c\tau$ of the b-hadrons are about 400 μm, 100 to 300 μm longer than the $c\tau$ of charmed-hadrons. Furthermore, the d_0 of b-hadrons daughters are larger than those of the tracks produced at the primary vertex as illustrated in Figure 1, but smaller than those of the long-lived K_s and Λ daughters. Therefore, the $L_{r\phi}$ and the track d_0 requirements remove contamination of short-lived charm hadrons, primary tracks, K_s and Λ, or secondary tracks from the particle interaction with the detector material.

From this "Two Track" dataset we reconstruct: 1. $\overline{B} \to \Lambda_c^+\mu^-X$ and $\Lambda_b \to \Lambda_c^+\pi^-$ where $\Lambda_c^+ \to pK^-\pi^+$, 2. $\overline{B} \to D^+\mu^-X$ and $\overline{B}^0 \to D^+\pi^-$ where $D^+ \to K^-\pi^+\pi^+$, 3. $\overline{B} \to D^{*+}\mu^-X$ and $\overline{B}^0 \to D^{*+}\pi^-$ where $D^{*+} \to D^0\pi^+$ and $D^0 \to K^-\pi^+$. Both the hadronic and semileptonic decays have four charged tracks in the final state. The tracks

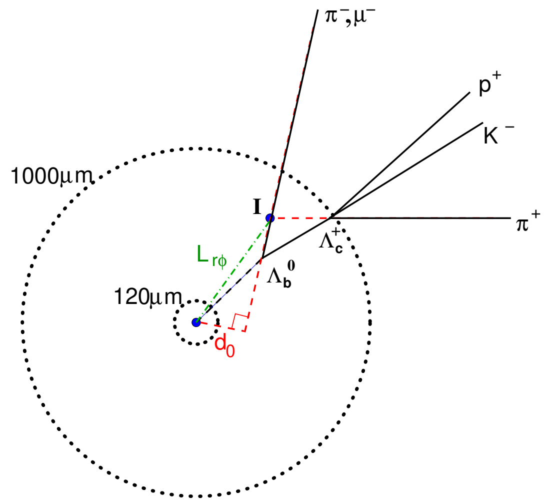

FIG. 1: Event topology in the plane transvers to the beam for a Λ_b decays reconstructed in this analysis. Definitions of impact parameter (d_0) and transverse displacement ($L_{r\phi}$) are indicated. The dashed circles indicate the requirements made by the trigger on d_0 and $L_{r\phi}$.

are required to have $P_T > 0.5$ GeV/c, at least 20 hits from the axial layers and the stereo layers of the Central Outer Tracker (COT), respectively, and at least 3 hits from the axial layers of the Silicon Vertex Detector (SVX). We further apply the kinematic requirements listed in Table I and impose that two out of the four charged tracks from the signal candidates pass the "Two Track" SVT trigger requirements. After applying all selection requrements, the number of signal events for each decay mode is obtained by fitting the b-hadron and charm hadron mass distributions. Because a neutrino is not reconstructed in the semileptonic decay, and the invariant mass of "charm+μ" is a broad spectrum with a shape poorly distinguished from the backgrounds, we extract $N_{\rm inc\,semi}$ in Equation 1 by fitting the "charm" mass spectrum and extract $N_{\rm had}$ by fitting the "charm+π" mass spectrum. Figure 2 shows the invariant mass spectra for the reconstructed signals with fits superimposed. Table II summarizes the signal yields for each decay mode returned from the fits.

III. MONTE CARLO AND DATA COMPARISON

We use the MC to obtain the efficiencies for the signals and the backgrounds. To confirm that the simulation accurately reproduces the data, we compare various reconstructed distributions from the MC with the same distributions from the data. For a fair comparison, the background present in the signal region of data must be removed. In the control samples, the combinatorial background dominates in the signal region and we perform a sideband subtraction to obtain a signal distribution, i.e. we subtract the histogram in the sideband region (4∼6 σ away from the mass mean) from the histogram in the signal region (2 σ around the mass mean) according to the ratio of the amount of backgrounds in these two regions.

The spectrum for produced Λ_b and $\overline{B}^0$ were each tuned to match the data. In addition, because a proper decay model for the Λ_b semileptonic decays is not implemented in the default decay package `EvtGen` [12] yet, we reweight the phase space distribution according to the form factor model in Huang [6] and the W spin effect from the decay package QQ [13]. Comparison of several important variables between MC and data are shown in Figure 3 after correcting the MC. Superimposed on the comparison plots are the probability that the data and MC distributions are compatable and indicate good agreement.

IV. BACKGROUNDS TO THE SEMILEPTONIC SIGNAL

The $\Lambda_c\mu$, $D\mu$ and $D^*\mu$ candidates we observe in the data consist of the exclusive semileptonic signals: $\Lambda_b \to \Lambda_c^+\mu^-\overline{\nu}_\mu$, $\overline{B}^0 \to D^+\mu^-\overline{\nu}_\mu$, $\overline{B}^0 \to D^{*+}\mu^-\overline{\nu}_\mu$, in the presence of other backgrounds. These backgrounds arise from three sources:

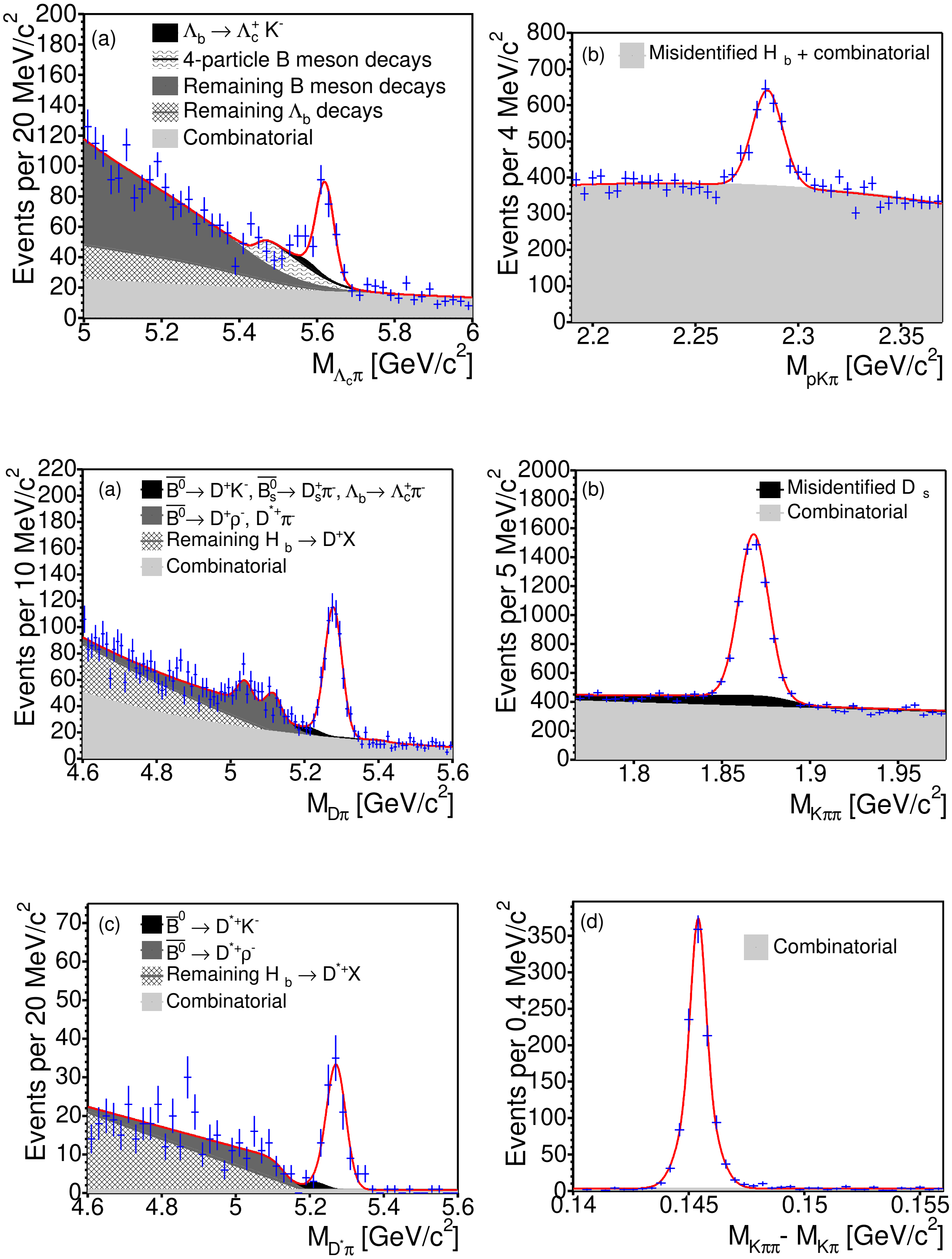

FIG. 2: "charm+π" and "charm" mass spectra from the data after all the selection requirements. From the top left to the bottom right are: $M_{\Lambda_c}\pi$, $M_{pK\pi}$, $M_{D\pi}$, $M_{K\pi\pi}$, $M_{D^*\pi}$ and $M_{D^0\pi} - M_{D^0}$. The results of the unbinned extended likelihood fits are superimposed on the histograms and a χ^2 probability is calculated.

TABLE I: Selection requirements for $\Lambda_b \to \Lambda_c^+ X$, $\overline{B} \to D^+ X$ and $\overline{B} \to D^{*+} X$ decays. Here, $\chi^2_{r\phi}$ is the χ^2 returned from a kinematic fit in the $r\phi$ plane. The π_B and μ_B are the π and μ from the decay of the parent b-hadron. The term "CMU fiducial" means that a track must extrapolate the fiducial region of the Central Muon Detector (CMU). The "CMU χ_x^2" is the matching χ^2 in the $r\phi$ plane between the extrapolated track and the hits in the CMU detector.

$\Lambda_b \to \Lambda_c^+ X$	$\overline{B} \to D^+ X$	$\overline{B} \to D^{*+} X$
$P_T(4_{\rm trks}) > 6$ GeV/c	$P_T(4_{\rm trks}) > 6$ GeV/c	$P_T(4_{\rm trks}) > 6$ GeV/c
$P_T(\Lambda_c) > 5$ GeV/c	$P_T(D) > 5$ GeV/c	$P_T(D^*) > 5$ GeV/c
$\chi^2_{r\phi}(4_{\rm trks}) < 15$	$\chi^2_{r\phi}(4_{\rm trks}) < 15$	$\chi^2_{r\phi}(4_{\rm trks}) < 17$
$\chi^2_{r\phi}(\Lambda_c) < 14$	$\chi^2_{r\phi}(D) < 14$	$\chi^2_{r\phi}(D^0) < 16$
$\frac{L_{r\phi}(4_{\rm trks})\cdot M_{\Lambda_b}}{P_T(4_{\rm trks})} > 250$ μm	$\frac{L_{r\phi}(4_{\rm trks})\cdot M_{B^0}}{P_T(4_{\rm trks})} > 200$ μm	$\frac{L_{r\phi}(4_{\rm trks})\cdot M_{B^0}}{P_T(4_{\rm trks})} > 200$ μm
$\frac{L_{r\phi}(\Lambda_c)\cdot M_{\Lambda_c}}{P_T(\Lambda_c)} >$ -70 μm	$\frac{L_{r\phi}(D)\cdot M_D}{P_T(D)} >$ -30 μm	$\frac{L_{r\phi}(D^0)\cdot M_{D^0}}{P_T(D^0)} >$ -70 μm
π_B and μ_B $P_T > 2.0$ GeV/c	π_B and μ_B $P_T > 2.0$ GeV/c	π_B and μ_B $P_T > 2.0$ GeV/c
π_B and μ_B CMU fiducial	π_B and μ_B CMU fiducial	π_B and μ_B CMU fiducial
π_B and μ_B 120 μm $< d_0 <$ 1000 μm	π_B and μ_B 120 μm $< d_0 <$ 1000 μm	π_B and μ_B 120 μm $< d_0 <$ 1000 μm
$P_T(p) > 2$ GeV/c	–	–
–	–	$1.833 < M_{K\pi} < 1.893$ GeV/c^2
	Semileptonic Mode	
μ_B CMU $\chi^2_x < 9$	μ_B CMU $\chi^2_x < 9$	μ_B CMU $\chi^2_x < 9$
3.7$< M_{\Lambda_c\mu} <$5.64 GeV/c^2	3.0$< M_{D\mu} <$5.3 GeV/c^2	3.0$< M_{D^*\mu} <$5.3 GeV/c^2
	Hadronic Mode	
2.269$< M_{pK\pi} <$2.302 GeV/c^2	$1.8517 < M_{K\pi\pi} < 1.8837$ GeV/c^2	$0.143 < M_{K\pi\pi} - M_{K\pi} < 0.148$ GeV/c^2

TABLE II: Observed number of events in each decay mode/reconstructed final state. The semileptonic final states may arise from multiple processes producing heavy flavor (b, c hadrons).

Mode	Yield
$\Lambda_b \to \Lambda_c^+\pi^-$	179 $\pm$ 19
$\Lambda_c^+\mu^- X$	1237 $\pm$ 97
$\overline{B}^0 \to D^+\pi^-$	579 $\pm$ 30
$D^+\mu^- X$	4720 $\pm$ 100
$\overline{B}^0 \to D^{*+}\pi^-$	106 $\pm$ 11
$D^{*+}\mu^- X$	1059 $\pm$ 33

- feed-in backgrounds: single b-hadron decays into similar final states, a charm hadron, a real muon and other tracks.
- false muons: a charm hadron and a track (p, K, π) with a large impact parameter which the muon requirements.
- $b\bar{b}$ and $c\bar{c}$: two b or charm hadrons from the $b\bar{b}$ and $c\bar{c}$ pairs decay into a D^* (D, Λ_c) and a muon, respectively.

The goal is to measure the relative branching fractions of the exclusive semileptonic decays to the hadronic decays. The backgrounds listed above should be subtracted from the observed inclusive semileptonic signal in the data. Equation 1

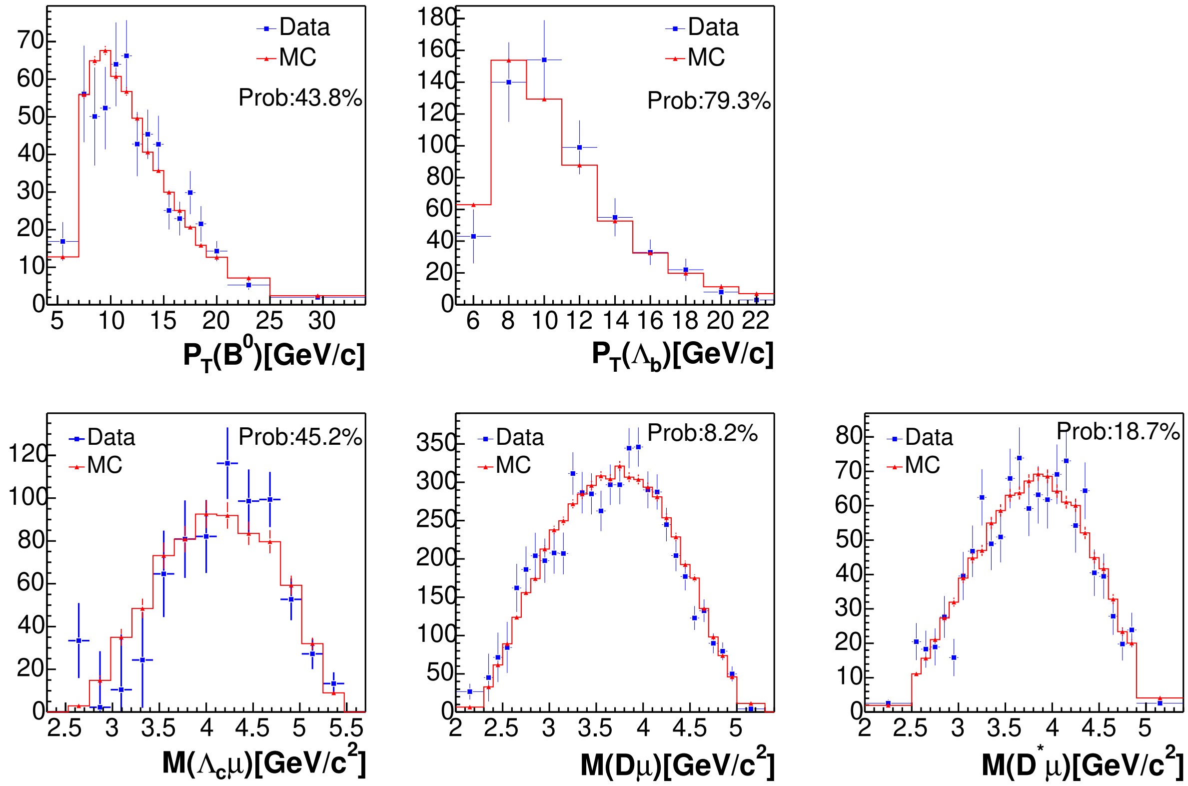

FIG. 3: MC (triangles) and data (squares) comparison. From the top left to the bottom right are: the transverse momentum (P_T) of the reconstructed B^0 from $\overline{B}^0 \to D^+\pi^-$ decays, P_T of the reconstructed Λ_b from $\Lambda_b \to \Lambda_c^+\pi^-$ decays, invariant mass of $\Lambda_c\mu$, $D\mu$ and $D^*\mu$. The semileptonic MC includes both the exclusive signal and associated backgrounds.

is then re-written as follows:

$$\frac{\mathcal{B}_{\text{semi}}}{\mathcal{B}_{\text{had}}} = \left(\frac{N_{\text{inclusive semi}} - N_{\text{feed}} - N_{\text{fake}\mu} - N_{b\bar{b},\, c\bar{c}}}{N_{\text{had}}}\right) \cdot \frac{\epsilon_{\text{had}}}{\epsilon_{\text{semi}}}. \tag{2}$$

We estimate $N_{\text{fake}\mu}$ by first reconstructing events with a charm hadron and a track that fails the muon identification requirements (TRK^{fail}) imposing the same selection criteria as was used for the signal reconstruction. Then, we weight the events that pass the selections with an average muon-fake probability ($\mathcal{P}_{\text{avg}}$) for the momentum and the charge of TRK^{fail}. The $N_{\text{fake}\mu}$ is extracted from a fit to the weighted charm mass distribution. The $\mathcal{P}_{\text{avg}}$ is the sum of the probability for a proton, kaon or pion to fake a muon each weighted by the fraction of tracks corresponding to a proton, kaon or pion. The fake probabilities come from measurements using pure samples of p, K and π. The fractions of protons, kaons and pions are obtained from the inclusive single b-generator MC [14].

We estimate the amount of the feed-in and $b\bar{b}$, $c\bar{c}$ backgrounds by normalizing them to the observed number of fully reconstructed hadronic signal events in the data:

$$N_{\text{feed}} = N_{\text{had}} \cdot \sum \frac{\mathcal{B}_i \cdot \epsilon_i}{\mathcal{B}_{\text{had}} \cdot \epsilon_{\text{had}}}, \tag{3}$$

$$N_{b\bar{b},c\bar{c}} = N_{\text{had}} \cdot \sum \frac{\sigma_{b\bar{b},c\bar{c}} \cdot \mathcal{B}_i \cdot \epsilon_i}{\sigma_{B^0,\Lambda_b} \cdot \mathcal{B}_{\text{had}} \cdot \epsilon_{\text{had}}}. \tag{4}$$

The efficiencies of the hadronic signal, in Equations 3–4 and the efficiencies of the feed-in backgrounds, in Equation 3, are obtained from either PYTHIA [15] MC for $b\bar{b}$ and $c\bar{c}$ backgrounds or a single b-generator [14] MC for all other backgrounds. The branching fractions are from the PDG, the `EvtGen` package [12], measurements at CDF-II and our estimates based on the HQET.

In order to reduce the uncertainty from Λ_b feed-in backgrounds, we search for resonances in our $\Lambda_c^+\mu$ events by combining a Λ_c^+ with one or two additional tracks. Each track is assigned a pion mass, required to have $p_T > 0.4$ GeV$/c$

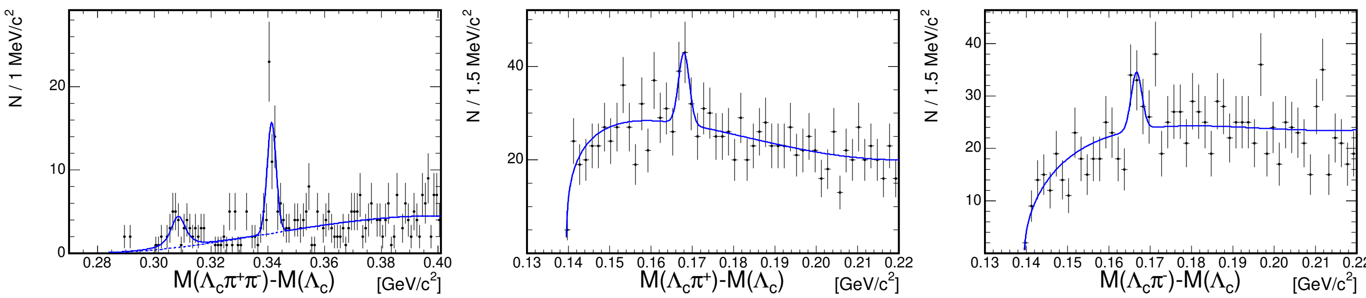

FIG. 4: Mass difference distributions for $\Lambda_c^+\pi^+\pi^-$(left), $\Lambda_c^+\pi^+$(middle) and $\Lambda_c^+\pi^-$(right) combinations. The peaks have mass differences which correspond to the $\Lambda_c(2595)^+$ and $\Lambda_c(2625)^+$ in the left plot, the $\Sigma_c(2455)^{++}$ in the middle plot and the $\Sigma_c(2455)^0$ in the right plot.

and be fiducal to the COT. By plotting the mass differences $(M_{\Lambda_c^+\pi^+} - M_{\Lambda_c^+})$, $(M_{\Lambda_c^+\pi^-} - M_{\Lambda_c^+})$, $(M_{\Lambda_c^+\pi^+\pi^-} - M_{\Lambda_c^+})$ we improve our mass resolution. Figure 4 shows the three mass difference distributions. Peaks are observed at mass differences corresponding to those expected for the $\Sigma_c(2455)^{++}$, $\Sigma_c(2455)^0$, $\Lambda_c(2595)^+$ and $\Lambda_c(2625)^+$. Fitting the mass difference distributions for a signal and background shape, gives the yields summarized in Table III. The yields for the two $\Sigma_c(2455)$ peaks have been corrected for the decay of the $\Lambda_c(2595)$ through a $\Sigma_c(2455)$ resonance in the Table. Then, correcting for acceptance, reconstruction efficiency and accounting for muon fakes allows us to measure the branching fractions relative to $\Lambda_b \to \Lambda_c^+\mu^-\overline{\nu}_\mu$:

$$\frac{\mathcal{B}(\Lambda_b \to \Lambda_c(2595)^+\mu^-\overline{\nu}_\mu)}{\mathcal{B}(\Lambda_b \to \Lambda_c^+\mu^-\overline{\nu_\mu})} = 0.126 \pm 0.033(\mathrm{stat})^{+0.047}_{-0.038}(\mathrm{syst}), \tag{5}$$

$$\frac{\mathcal{B}(\Lambda_b \to \Lambda_c(2625)^+\mu^-\overline{\nu}_\mu)}{\mathcal{B}(\Lambda_b \to \Lambda_c^+\mu^-\overline{\nu_\mu})} = 0.210 \pm 0.042(\mathrm{stat})^{+0.071}_{-0.050}(\mathrm{syst}), \tag{6}$$

$$\frac{\mathcal{B}(\Lambda_b \to \Sigma_c(2455)\pi\mu^-\overline{\nu}_\mu)}{\mathcal{B}(\Lambda_b \to \Lambda_c^+\mu^-\overline{\nu_\mu})} = 0.054 \pm 0.022(\mathrm{stat})^{+0.021}_{-0.018}(\mathrm{syst}). \tag{7}$$

where we've assumed isospin symmetry for the decays involving a $\Sigma_c(2455)$:

$$\mathcal{B}(\Lambda_b \to \Sigma_c(2455)^{++}\pi^-\mu^-\overline{\nu}_\mu) = \mathcal{B}(\Lambda_b \to \Sigma_c(2455)^+\pi^0\mu^-\overline{\nu}_\mu) = \mathcal{B}(\Lambda_b \to \Sigma_c(2455)^0\pi^+\mu^-\overline{\nu}_\mu). \tag{8}$$

TABLE III: Observed number of signal events, corresponding significance and fitted mass diffferences in the data for each Λ_b semileptonic decay mode.

Mode	Yield	Significance	$\Delta M[\mathrm{MeV}/c^2]$
$\Lambda_c(2595)^+\mu^-X$	$31 \pm 8(\mathrm{stat}) \pm 7(\mathrm{syst})$	2.9	$308.47 \pm 0.99(\mathrm{stat})$
$\Lambda_c(2625)^+\mu^-X$	$53 \pm 9(\mathrm{stat}) \pm 5(\mathrm{syst})$	5.2	$341.39 \pm 0.31(\mathrm{stat})$
$\Sigma_c(2455)^{++}\pi^-\mu^-X$	$16 \pm 11(\mathrm{stat}) \pm 7(\mathrm{syst})$		$166.72 \pm 0.69(\mathrm{stat})$
$\Sigma_c(2455)^0\pi^+\mu^-X$	$26 \pm 12(\mathrm{stat}) \pm 9(\mathrm{syst})$		$168.01 \pm 0.51(\mathrm{stat})$
$\Sigma_c(2455)$ modes combined		2.1	

We obtain the absolute branching fractions of these Λ_b decays by multiplying the ratios with the estimated $\mathcal{B}(\Lambda_b \to \Lambda_c^+\mu^-\overline{\nu}_\mu)$. We estimate $\mathcal{B}(\Lambda_b \to \Lambda_c^+\mu^-\overline{\nu}_\mu)$ by taking a weighted average of $\mathcal{B}(\overline{B}^0 \to D^+\mu^-\nu) + \mathcal{B}(\overline{B}^0 \to D^{*+}\mu^-\nu) =$ and scale that number by the ratio of lifetimes, $\frac{\tau_{\Lambda_b}}{<\tau_{B^0}>} = 0.99 \pm 0.10$, and estimate $\mathcal{B}(\Lambda_b \to \Lambda_c^+\mu^-\overline{\nu}_\mu) = 7.3 \pm 0.8 \pm 1.1\%$. The fraction of each type of background in the inclusive semileptonic signal is summarized in Table IV. The feed-in background dominates followed by the background from muon fakes. The smallest background source is from $b\overline{b}$ and $c\overline{c}$.

TABLE IV: Summary of the backgrounds to the semileptonic modes.

	$N_{\rm bg}/N_{\rm inc\ semi}$ (%)		
Source	$\Lambda_c\mu$	$D\mu$	$D^*\mu$
Signal	72.5	55.5	73.7
Feed-in	24.0	38.0	20.8
Muon fakes	3.2	4.9	4.2
$b\bar{b}$ and $c\bar{c}$	0.3	1.6	1.3

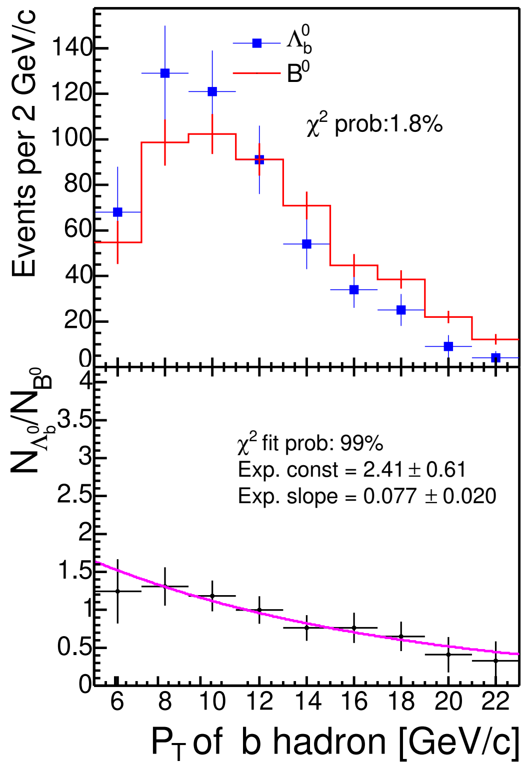

FIG. 5: Comparison of the measured P_T spectra for the Λ_b and B^0 where the B^0 spectrum is normalized to Λ_b spectrum (top) and the ratio of the two spectra is shown in the bottom.

A. Corrections for $\frac{\sigma_{\Lambda_b}}{\sigma_{B^0}}$ and Derivation of $\mathcal{B}(\Lambda_b \to \Lambda_c^+\pi^-)$

While precise measurements of $\mathcal{B}(\overline{B}^0 \to D^{*+}\pi^-)$ and $\mathcal{B}(\overline{B}^0 \to D^+\pi^-)$ exist [8], there is not yet a direct measurement of $\mathcal{B}(\Lambda_b \to \Lambda_c^+\pi^-)$. The CDF Run II measurement of $\frac{\sigma_{\Lambda_b}(P_T>6.0)\mathcal{B}(\Lambda_b\to\Lambda_c^+\pi^-)}{\sigma_{B^0}(P_T>6.0)\mathcal{B}(\overline{B}^0\to D^+\pi^-)}$ by Le, *et al.* [16] provides an input but requires understanding of the production cross section. Since no production cross section measurements exist for the Λ_b, one must infer the cross-section using other means. From the total b-quark cross-section [9], the fragmentation fraction (f_u, f_d, f_s and $f_{\rm baryon}$), and assuming the composition of the b-baryons is dominated by Λ_b, i.e. $f_{\Lambda_b} \cong f_{\rm baryon}$, we may infer the production cross-section of any b-hadron species, *e.g*: $\sigma_{\Lambda_b} = \sigma_b \cdot f_{\rm baryon}$. However, the fragmentation fractions assume that either the entire P_T spectrum is measured for both B^0 and Λ_b in the above ratio or the two P_T spectra are the same. Most analyses at CDF require a P_T threshold to improve the signal to background ratio. Any difference in the P_T spectrum between B^0 and Λ_b will modify the effective fragmentation fraction. Moreover, if the P_T spectrum used in the MC is incorrect, the kinematic acceptance will be over- or under-estimated.

The PDG [8] determines $f_{\rm baryon}$ by combining the measurements of mean lifetimes, B^0 mixing parameters and branching ratios by LEP, SLD and Taylor in CDF-I [18]. Nevertheless, it is questionable whether the $f_{\rm baryon}$ should be the same for the LEP and the Tevatron experiments. Because the collider and the detector environments for

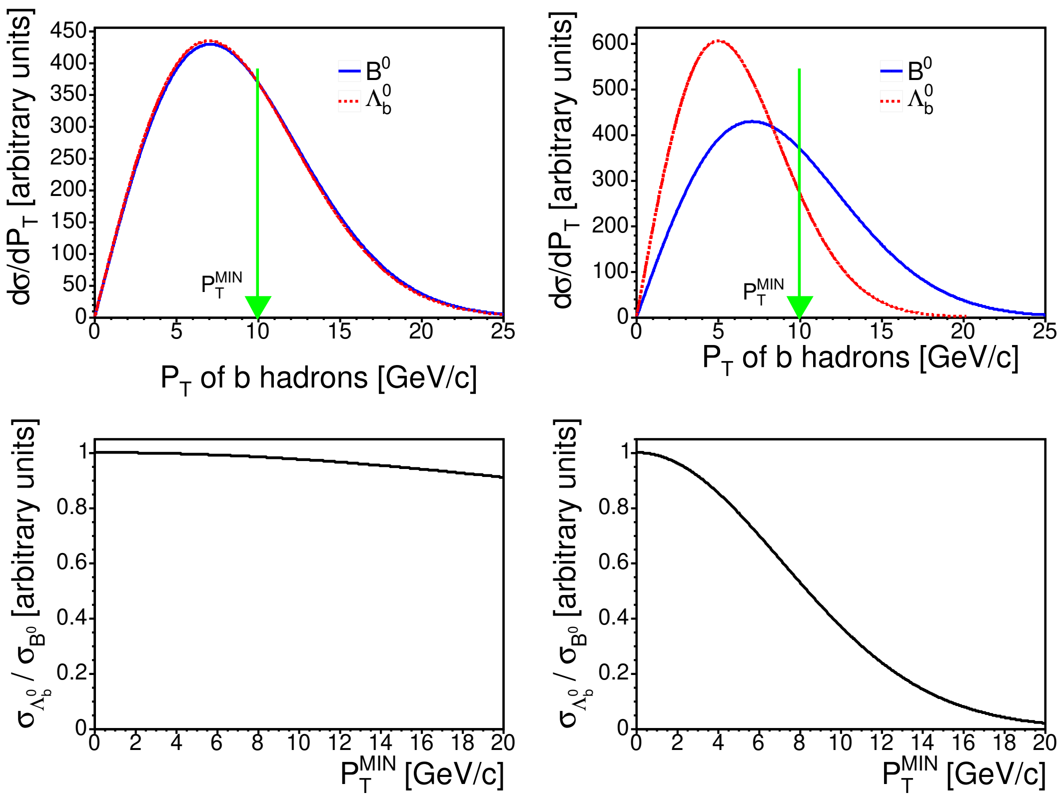

FIG. 6: Cartoon illustrating similar (left) and different (right) P_T specta for Λ_b and B^0. Production cross sections measured above some P_T threshold (P_T^{MIN}) are proportional to the area to the right of the arrows. The bottom figures show the ratio of cross sections as a function of P_T^{MIN}.

Taylor's analysis are most similar to those for this analysis and we have access to the details of the measurement of f_{baryon}/f_d with corrections for differences between Taylor's and our experimental conditions. As accurate Λ_b and B^0 P_T spectra from the fully reconstructed decays were not available for CDF-I, we first correct the kinematic acceptance in Taylor [18] using the MC produced with the measured Λ_b and B^0 P_T spectra (see Section III and Figure 5). Because, the ratio of the fragmentation fractions, or $\frac{\sigma_{\Lambda_b}}{\sigma_{B^0}}$, depends on the value of P_T threshold. The P_T threshold in Taylor [18] is 10 GeV/c, tighter than the 6 GeV/c threshold in our analysis. Consequently, we convert the effective fragmentation fractions between the two thresholds, by integrating the raw P_T spectrum from each threshold to infinity and calculating the ratio of the two areas as illustrated in Figure 6. A final correction is applied to account for the difference in the $\mathcal{B}(\Lambda_b \to \Lambda_c^+\mu^-\overline{\nu}_\mu)$ between Taylor's and our analyses. After corrections of the kinematic acceptance and the P_T threshold and branching fraction, we insert the corrected $\frac{\sigma_{\Lambda_b}}{\sigma_{B^0}}$ and $\mathcal{B}(\overline{B}^0 \to D^+\pi^-)$ into Le's result, and find

$$\mathcal{B}(\Lambda_b \to \Lambda_c^+\pi^-) = \left(0.36\ ^{+0.24}_{-0.17}\ (stat \oplus syst)^{+0.05}_{-0.07}\ (P_T \text{ spectrum})\right)\%, \tag{9}$$

which is in good agreement with the prediction by Leibovich, *et al.* [7], 0.54%. The last uncertainty is due to the size of the sample for measuring the Λ_b P_T spectrum.

V. SYSTEMATIC UNCERTAINTIES

Systematic uncertainties in this analysis may be broken down into three categories; internal systematic uncertainties, uncertainties from external measurements summarized by the particle data group (PDG) and estimates of branching fractions which have not yet been measured (EBR). Internal systematic uncertainties arise from the models used in fitting the b and charm hadron mass distributions, uncertainties on the muon fake estimates and modelling of geometric and kinematic acceptances and are unique to this measurement. External systematic uncertainties are related to the precision of external input. For each source of systematic uncertainty, we vary the source of the uncertainty by $\pm$ one standard deviation and quote the difference between the new relative branching fractions with the central value. Each uncertainty is discussed for the Λ_b result below. Systematic uncertainties for the $\overline{B}^0$ results are obtained in a similar fashion.

The uncertainty from the mass fitting model is studied by varying the parameter left constant in the fit $\pm$ 1 estimated standard deviation for that parameter. Background shapes which depend on branching fractions of various b hadron decay modes have each branching fraction varied independently within its uncertainty. The uncertainty of the fake muon estimate comes from the sample size of the measurements that determine the muon fake probability, the fit to the weighted charm hadron mass distribution, and the uncertainties on the p, K, π fractions due to the uncertainties on the branching fractions for the decays in the inclusive MC sample. MC modeling of geometrical and kinematic acceptance include effects of the measured P_T spectrum, efficiency scaling factor to account for the difference between MC and data, modeling of the QCD processes, material in the detector simulation, Λ_c Dalitz structure, Λ_b lifetime, Λ_b and Λ_c polarizations, and Λ_b semileptonic decay model. The size of the data sample used in the measurements of the P_T spectra and efficiencies, affects the uncertainties on the data/MC ratio. We vary the ratio $\pm$ 1 σ to assign the systematic uncertainty. We assign 100% uncertainty to the amount of $b\bar{b}$ and $c\bar{c}$ backgrounds, due to our lack of knowledge of the relative $b\bar{b}$ and $c\bar{c}$ production rates between different QCD processes. The uncertainty from the detector material is studied by switching off the hadronic interaction in the detector simulation and multiply the difference from the central value with 25%. The 25% is a quadrature sum of the 15% underestimate in the amount of detector material and the 20% due to the difference between the default hadronic interaction model, `GHEISHA`, and the other model, `FLUKA` [19, 20]. The effect of the Λ_c Dalitz structure is studied by varying branching ratios of the resonant and non-resonant $\Lambda_c \to pK\pi$ decays measured by E791 [21]. The Λ_b lifetime is varied by the uncertainty on the world average. The effect of the polarizations is studied by reweighting the angular distribution in the MC according to the Λ_b and Λ_c polarization states: $\pm$ 1, since the Λ_b and Λ_c are produced unpolarized in the MC. Systematic uncertainty from the Λ_b decay model is dominated by the statistics of the independent MC sample used for reweighting the phase space distribution (see Section III). The leading CDF internal systematic uncertainties are from the mass fitting model, measured P_T spectrum for both the B^0 results with a significant contribution from the the Λ_b semileptonic decay model for the Λ_b result. Uncertainties on the measured branching fractions come from the PDG and include those of the newly observed Λ_b semileptonic decays in this analysis (see Section IV). For the estimated branching fractions, we assign a 5% uncertainty to the estimated branching fractions of the excited charm meson decays and a 100% uncertainty to the estimated branching fractions of the b hadron decays. Because the excited charm hadrons decay via the strong interaction and conserve isospin symmetry, their branching fractions can be inferred from Clebsch-Gordan Coefficients. While for the weak decays of b hadrons, the allowable decay spectrum is wider. Table V summarizes the systematic uncertainties for this analysis. The dominant uncertainties for $\mathcal{B}(\Lambda_b \to \Lambda_c^+\pi^-)$ arise from $\frac{\sigma_{\Lambda_b}}{\sigma_{B^0}}$ and $\mathcal{B}(\Lambda_c^+ \to pK^-\pi^+)$.

VI. RESULTS

For the control modes, we measure the relative branching fractions to be:

$$\frac{\mathcal{B}(\overline{B}^0 \to D^+\mu^-\overline{\nu}_\mu)}{\mathcal{B}(\overline{B}^0 \to D^+\pi^-)} = 9.9\ \pm 1.0\ (stat) \pm 0.6\ (syst) \pm 0.4\ (PDG) \pm 0.5\ (EBR),$$

and

$$\frac{\mathcal{B}(\overline{B}^0 \to D^{*+}\mu^-\overline{\nu}_\mu)}{\mathcal{B}(\overline{B}^0 \to D^{*+}\pi^-)} = 16.5\ \pm 2.3\ (stat) \pm 0.6\ (syst) \pm 0.5\ (PDG) \pm 0.8\ (EBR),$$

We then measure the relative Λ_b branching fraction to be:

$$\frac{\mathcal{B}(\Lambda_b \to \Lambda_c^+\mu^-\overline{\nu}_\mu)}{\mathcal{B}(\Lambda_b \to \Lambda_c^+\pi^-)} = 16.6\ \pm 3.0\ (stat) \pm 1.0\ (syst)^{+2.6}_{-3.4}\ (PDG) \pm 0.3\ (EBR).$$

The uncertainties of the relative branching fractions are from statistics, CDF internal systematics, external measured branching ratios and unmeasured branching ratios, respectively.

The results for the ratio of branching fractions for the B^0 are consistent with the ratios obtained by the PDG, 8.10 ± 0.60 and 18.70 ± 0.97 at the 1.3 and 0.8 σ level. The result for the ratio of branching fractions for the Λ_b are consistent with predictions by Leibovich,*et al.* and Huang, *et al.*

TABLE V: Summary of statistical and systematic uncertainties. The σ_R is uncertainty on the relative branching fraction, R.

Source	$\frac{\sigma_R}{R}$ (%) $\frac{\mathcal{B}(\Lambda_b\to\Lambda_c^+\mu^-\overline{\nu}_\mu)}{\mathcal{B}(\Lambda_b\to\Lambda_c^+\pi^-)}$	$\frac{\mathcal{B}(\overline{B}^0\to D^+\mu^-\overline{\nu}_\mu)}{\mathcal{B}(\overline{B}^0\to D^+\pi^-)}$	$\frac{\mathcal{B}(\overline{B}^0\to D^{*+}\mu^-\overline{\nu}_\mu)}{\mathcal{B}(\overline{B}^0\to D^{*+}\pi^-)}$
Mass fitting	$^{+3.8}_{-3.1}$	4.1	< 0.1
P_T spectrum	$^{+0.0}_{-2.9}$	3.0	2.4
detector material	1.3	1.7	1.3
Fake μ	1.0	0.7	0.4
efficiency scaling factor	0.4	0.5	0.4
$b\overline{b}$, $c\overline{c}$	0.3	2.9	1.7
MC sample size	2.0	1.6	1.7
Λ_b, Λ_c polarizations	2.2	–	–
Λ_c Dalitz	0.4	–	–
Λ_b lifetime	0.3	–	–
Λ_b decay model	3.3	–	–
Total CDF internal	6.3	6.3	3.7
PDG	$^{+15.6}_{-20.4}$	4.1	2.8
Estimated $\mathcal{BR}$	2.1	4.7	4.9
Statistical	17.8	9.7	14.1

VII. CONCLUSION

We analyze 172 pb^{-1} of data collected with the CDF-II detector in the $p\overline{p}$ collisions at $\sqrt{s} = 1.96$ TeV. Using a novel secondary vertex track trigger, we reconstruct 1237 ± 97 $\overline{B} \to \Lambda_c^+\mu^- X$ decays and 179 ± 19 $\Lambda_b \to \Lambda_c^+\pi^-$ decays. The large sample of Λ_b enables us to measure the relative Λ_b branching fractions and examine the Heavy Quark Effective Theory. We have also observed several Λ_b semileptonic decays which have never been seen in the other experiments: $\Lambda_b \to \Lambda_c(2595)^+\mu^- X$, $\Lambda_b \to \Lambda_c(2625)^+\mu^- X$, $\Lambda_b \to \Sigma_c(2455)^0\pi^+\mu^- X$, and $\Lambda_b \to \Sigma_c(2455)^{++}\pi^-\mu^- X$. In addition, we reconstruct the $\overline{B}^0 \to D^{*+}$ and $\overline{B}^0 \to D^+$ decays similar to our Λ_b decays and use them as the control samples to understand the issues associated with the Λ_b measurement. After the estimate and the subtraction of the background in the inclusive semileptonic signal, we correct the yield observed in the data with the trigger and reconstruction efficiencies obtained from the Monte Carlo. We find the relative branching fraction of the control modes in good agreement with the values obtained by the PDG. We measure the ratio of Λ_b branching fraction to be:

$$\frac{\mathcal{B}(\Lambda_b \to \Lambda_c^+\mu^-\overline{\nu}_\mu)}{\mathcal{B}(\Lambda_b \to \Lambda_c^+\pi^-)} = 16.6 \pm 3.0(stat) \pm 1.0(syst)^{+2.6}_{-3.4}(PDG) \pm 0.3(EBR).$$

The uncertainty is dominated by the size of the data sample and the branching ratio of $\Lambda_c^+ \to pK^-\pi^+$. More data and a more precise measurement of $\mathcal{B}(\Lambda_c^+ \to pK^-\pi^+)$ in the future will immediately improve our relative branching fraction measurement and our determination of $\mathcal{B}(\Lambda_b \to \Lambda_c^+\mu^-\overline{\nu}_\mu)$.

Acknowledgments

We thank the Fermilab staff and the technical staffs of the participating institutions for their vital contributions. This work was supported by the U.S. Department of Energy and National Science Foundation; the Italian Istituto Nazionale di Fisica Nucleare; the Ministry of Education, Culture, Sports, Science and Technology of Japan; the Natural Sciences and Engineering Research Council of Canada; the National Science Council of the Republic of China; the Swiss National Science Foundation; the A.P. Sloan Foundation; the Bundesministerium fuer Bildung und Forschung, Germany; the Korean Science and Engineering Foundation and the Korean Research Foundation; the

Particle Physics and Astronomy Research Council and the Royal Society, UK; the Russian Foundation for Basic Research; the Comision Interministerial de Ciencia y Tecnologia, Spain; and in part by the European Community's Human Potential Programme under contract HPRN-CT-20002, Probe for New Physics.

[1] N. Cabibbo, Phys. Rev. Lett. **10**, 53 (1963).
[2] M. Kobayashi, T.Maskawa, Prog. Theor. Phys. **49**, 652 (1973).
[3] A. V. Manohar and M. B. Wise, Camb. Monogr. Part. Phys. Nucl. Phys. Cosmol. **10**, 1 (2000).
[4] N. Isgur, D. Scora, B. Grinstein and M. B. Wise, Phys. Rev. D **39**, 799 (1989).
[5] S. Godfrey and N. Isgur, Phys. Rev. D **32**, 189 (1985).
[6] M. Q. Huang, H. Y. Jin, J. G. Korner and C. Liu,
[7] A. K. Leibovich, Z. Ligeti, I. W. Stewart and M. B. Wise, Phys. Lett. B **586**, 337 (2004) [arXiv:hep-ph/0312319].
[8] C. Amsler, *et al.* [Particle Data Group], Phys. Lett. B **667**,1 (2008).
[9] D. Acosta *et al.* [CDF Collaboration], Phys. Rev. D **71**, 032001 (2005) [arXiv:hep-ex/0412071].
[10] B. Ashmanskas *et al.* [CDF-II Collaboration], Nucl. Instrum. Meth. A **518**, 532 (2004) [arXiv:physics/0306169].
[11] The $r\phi$ plane is the transverse plane perpendicular to the beam line.
[12] D. J. Lange, Nucl. Instrum. Meth. A **462**, 152 (2001).
[13] P. Avery, K. Read and G. Trahern, CLEO Software Note CSN-**212**
[14] K. Anikeev, P. Murat and C. Paus, CDF internal note **CDF5092** August 1999.
[15] T. Sjostrand et al., High-Energy-Physics Event Generation with PYTHIA 6.1, Comput. Phys. Commun. **135**, 238 (2001).
[16] Y. Le, M. Martin, and P. Maksimović, Phys. Rev. Lett. **98**, 122002 (2007).
[17] D. Abbaneo *et al.* [ALEPH Collaboration], arXiv:hep-ex/0112028.
[18] T. Affolder *et al.* [CDF Collaboration], Phys. Rev. Lett. **84**, 1663 (2000) [arXiv:hep-ex/9909011].
[19] R. Brun, R. Hagelberg, M. Hansroul, and J.C. Lassalle, CERN-DD-**78-2**-REV
[20] D. Michael, NuMI-NOTE-BEAM-**0019**
[21] E. M. Aitala *et al.* [E791 Collaboration], Phys. Lett. B **471**, 449 (2000) [arXiv:hep-ex/9912003].